

Silicic Volcanism in the Lunar Compton-Belkovich Volcanic Complex and Near-side Calderas

Elena Carlson, Shaughnessy Dunn, Taylor Hagerman, and Izzy Perez^a

^aUniversity of Colorado, Boulder, CO,

Abstract

This study explores the presence and origin of silicic volcanism on the Moon, an unexpected phenomenon given the lunar surface's lack of water and plate tectonics—two key processes in our understanding of silicic magma formation on Earth. We analyzed the spectra, gravitational anomalies, albedo, and abundance of KREEP (potassium, rare earth elements, and phosphorus) elements in regions with observed silicic volcanism, including the Compton-Belkovich Volcanic Complex and the near-side calderas of Mare Nectaris and Mare Imbrium. Spectral and elemental abundance analysis confirmed the existence of large amounts of silicic materials in each studied region. Through comparing the spectra of each region to lab-derived spectral data of common compounds found in basaltic and silicic magma, we were able to better understand the overall composition of these volcanic regions. Further analysis of KREEP elemental abundances in each region provided a strong justification for the importance of KREEP elements in silicic magma formation. Correlations between gravity and albedo, along with positive subsurface gravitational differences, confirmed significant interior composition differences that also support the presence of silicic volcanism and indicate subsurface features existing in these regions. Our results enhance our understanding of the processes beneath the Moon's surface that allow for partial heating of crustal material, leading to the formation of silicic magma and thus silicic volcanism. Our research enriches our knowledge of early lunar geology and therefore planetary volcanic activity.

Keywords: silicic volcanism, KREEP, gravitational anomalies, partial heating

1. Introduction

1.1. Silicic Volcanism

In the ongoing study of the lunar surface and the origin of volcanic features, there has been spectroscopic data indicating silicic volcanism. Silicic volcanism refers to volcanic activity that has magma with high silica content. These features were initially detected through remote sensing data by Whitaker in 1972, and were characterized by deep ultraviolet absorptions, low FeO and TiO₂ abundances, and high-thorium (Glotch et al. (2010); Qiu et al. (2023)). These areas of silicic volcanism are known as spectral “red spots” and have other similarities such as high albedos and morphological characteristics such as domes with steep slopes (Glotch et al. (2010); Valencia et al. (2021)). Silicic volcanism on the Moon is of particular interest in the scientific community because its formation remains poorly understood.

More commonly seen on the Moon is iron-rich or basaltic volcanism, as this is a simpler process of single-stage melting of mantle rock (Siegler et al. (2023)). These silica enriched materials have previously been observed on and beneath the surface of structures known as volcanic domes, which have formed after volcanic eruptions of silicic-rich magma (Wilson & Head (2003); Qiu et al. (2023)).

On Earth, both plate tectonics and the presence of water inside of rocks fosters silicic magma formation. Given the Moon's lack of water and plate tectonics we hope to provide some insight to the origin of these volcanoes. By looking at the

abundance and distribution of silica materials in specific lunar regions it may shed light on the potential processes that could lead to the formation of silica materials and provide a better understanding of planetary geology in general.

1.2. KREEP Elements and Gravitational Anomalies in the CBVC and the Near-side Caldera

For our research to provide accurate results on the formation of silicic volcanoes on the lunar surface, we need to conduct analysis on various areas such as the Compton-Belkovich Volcanic Complex (CBVC) and two near-side calderas, Mare Imbrium, and Mare Nectaris. Many previous studies focus on the CBVC and the potential for partial remelting of KREEP elements within the crust as an explanation for silicic lunar magmatism in the absence of plate tectonics and water (Siegler et al. (2023); Jolliff et al. (2011); Wilson & Head (2003)). In 2023, Su conducted phase equilibrium modeling of lunar igneous rocks which indicated that KREEP and Ti-high basalts have more silica-fertile characteristics than other rocks.

Another region that has been a focus of study for understanding the origins of silicic volcanism is the Procellarum KREEP Terrane (PKT), which has low elevations, thin crust and high surface concentrations of potassium and thorium (Glotch et al. (2010); Andrews-Hanna et al. (2014)). Mare Imbrium lies in the northeast of this region and has interesting topographic features that point to silicic volcanism (Ivanov et al. (2016)), giving us a good starting point for research into this region. The

other mare we chose was Mare Nectaris, which is further along the outskirts of the PKT; not much research has been focused towards this area which will allow us to see if there are similarities between these two near-side caldera that prove the origin of silicic volcanism on the Moon.

The partial melting of the crust is most likely driven by internal radiogenic heating where KREEP-rich magmas are buried under the crust at shallow depths (Su (2023)). Differences in subsurface density that have been observed through gravity analysis indicate multiple phases of silicic volcanism have taken place (Qiu et al. (2023)). Multiple phases of reheating crustal layers of radiogenic material formed by a long-lived thermal source can form silicic magma (Siegler et al. (2023)) which can be detected near the CBVC and Mare Imbrium (Qiu et al. (2023); Siegler et al. (2023); Ivanov et al. (2016)).

In this study, we analyzed spectral data and gravitational anomalies to investigate the origins of silicic magmatism in our chosen regions. Using gravitational data to study density differences in the surrounding craters and volcanic domes will show evidence of multiple layers of chambers that in the past would be sources of internal radiogenic heating, by studying the spectra and abundance of KREEP elements and thorium in these regions we have been able to show that the high abundance of these materials indicate their involvement in silicic magma formation. Conducting our studies on these various mares and the CBVC will diversify our region of study to produce precise results.

2. Methods

2.1. Regions of Interest

We chose to analyze two general regions on the Moon, the CBVC (Figure 1) and the PKT. Within the PKT, we looked at Mare Imbrium and Mare Nectaris (Figures 2 and 3 respectively). These regions were chosen based on previous studies which analyzed silicic volcanism at each site. (eg. Siegler et al. (2023); Jolliff et al. (2011); Wilson et al. (2014)). These past studies indicate that silicic volcanic activity likely occurred, however our spectral analysis checks this assumption before proceeding further to analyze KREEP element abundance as well as gravity and albedo data.

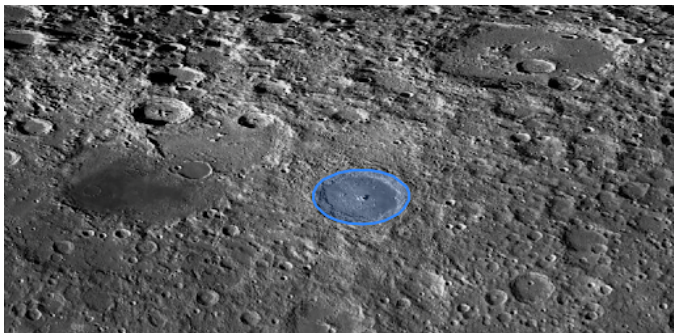


Figure 1: The Compton-Belkovich Volcanic Complex (CBVC) is highlighted in blue in this image. The center coordinates of this region are 60.5°N , 99.5°E . The image was obtained from the Wide Angle Camera (WAC) aboard the Lunar Reconnaissance Orbiter (LRO).

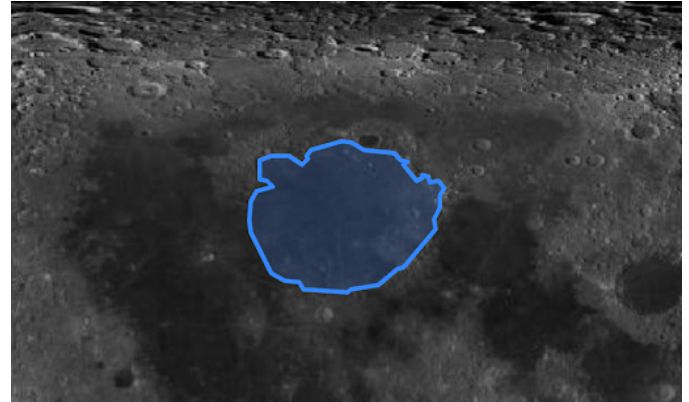


Figure 2: Mare Imbrium is highlighted in blue in this figure. The center coordinates of this region are 32.8°N , 15.6°E . The image was obtained from the Wide Angle Camera (WAC) aboard the Lunar Reconnaissance Orbiter (LRO).

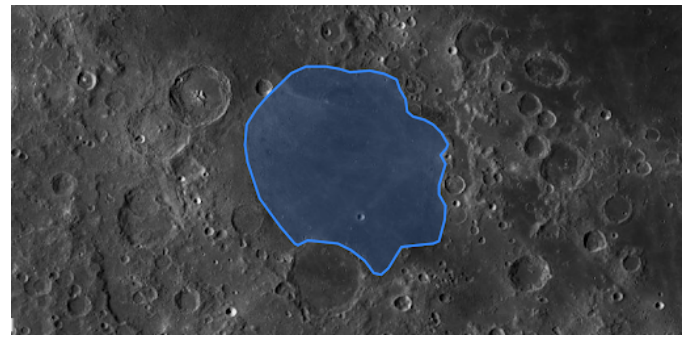


Figure 3: Mare Nectaris is highlighted in blue in this figure. The center coordinates of this region are -15.9°N , 34.6°E . The image was obtained from the Wide Angle Camera (WAC) aboard the Lunar Reconnaissance Orbiter (LRO).

2.2. Gravity and Albedo

Based on previous publications, we knew there would be large gravitational differences resulting from Gravity Recovery and Interior Laboratory (GRAIL) data that indicated a large difference from the expected to measured gravity. This indicates that there are density features beneath the surface that are unexpected, causing gravitational differences. We also analyzed these areas for their albedos. This was an important correlation to identify because silicic materials are highly reflective. By proving that there is a peak in albedo in these areas compared to surrounding areas, we can assume that there is a strong presence of silicic materials. It was important that the measured large gravitational differences be in the same locations as higher albedo measurements in order to confirm that there are unexpected subsurface features such as plutons from silicic volcanism.

The GRAIL data was downloaded from the Planetary Data System archive as an image file (3D array of longitude, latitude, and value of gravity in the z-direction). The albedo data was also downloaded from the Lunar Orbiter Laser Altimeter (LOLA) mission as an image file. In order to compare the data sets together and ensure they were the same shape, we interpolated them to be on the same latitude and longitude grid. We then isolated the data from each image to our regions of interest.

From those isolated regions, we normalized their distributions for gravity and albedo and displayed the data as a histogram. The mean, μ , and standard deviation, σ , were calculated for each data set and each region.

2.3. Spectral Analysis

To test that silicic volcanism was once present on the Moon, we looked at the Compton-Belkovich Volcanic Complex and the Procellarum KREEP Terrane which includes Mare Imbrium and Mare Nectaris. These are two priorly studied regions that have indicators of silicic volcanism. To retest this hypothesis, we chose to analyze lab spectra from Brown RELAB. Specifically, we looked at the spectra of tectosilicate plagioclase feldspar, iron oxide, olivine, and augite. We looked at the reflectivity of wavelengths ranging from the far-UV to the near-infrared. This data was in a text file format, with data on wavelength, corresponding reflectivity values, and error.

We then plotted reflectivity data from the Compton-Belkovich region of the Moon (60.5°N , 99.5°E). The reflectivity data was obtained via the Moon Mineralogy Mapper database and was in the form of image files and included reflectivity for a range of 85 bands each corresponding to different wavelengths once again spanning the far-UV to the near-infrared. To find the data that corresponded to our specific lunar regions of interest, we used the Lunar Orbital Data Explorer (ODE) to find radiance files corresponding to the specific longitude and latitude values. We then found the corresponding reflectance file to analyze reflectance values in this area.

When plotting the spectra against one to another, we first normalized the data by dividing all reflectance values by the reflectance values at a specific wavelength. In this case, we chose 989 nanometers to be the normalization wavelength. Following normalization, we interpolated the lab spectral reflectance values onto the Moon Mineralogy Mapper wavelengths to ensure that all data arrays were the same length. Using a least-squares minimization regression modeling, we were able to determine the mixing coefficients of the data.

2.4. KREEP Elements

To test for the existence and concentration of KREEP elements at our specific lunar regions, we analyzed thorium and potassium from the Lunar Prospector (LP) Reduced Spectrometer Data. The downloaded data files were in the form of text files with columns indicating minimum and maximum longitude and latitude values, and parts per million (PPM) of the indicated elements. Using Python, we were able to narrow down the large quantity of data to only points within our specific regions of interest. We then produced a colormap scatter plot of PPM versus location for each of our regions. We used the same technique as above to analyze the abundance of silicon and oxygen at each of our regions.

3. Results and Figures

3.1. Gravity and Albedo

We first wanted to illustrate how the measured gravity and albedo of the lunar surface differ across the various surface fea-

tures of the Moon (Figures 4 and 5 respectively). Following our gravitational analysis, we found the mean and standard deviation of gravitational (Table 1) and albedo (Table 2) differences for each region, which was then plotted to show the distribution of our results (Figures 6.e-6.j). From our analysis we were able to illustrate the correlations between positive gravity anomalies and albedo in each of our regions of interest (Figures 6.a-6.c).

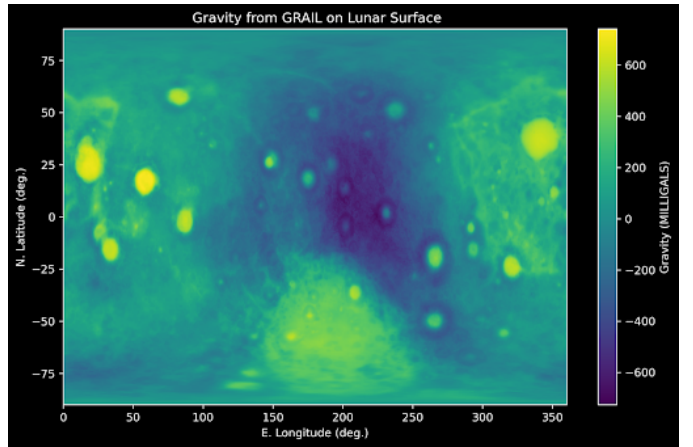


Figure 4: This figure is visual representation of the measured gravity across the lunar surface. The x and y axes correspond to degrees of longitude and latitude respectively while the colorbar represents the gravity strength in milligals.

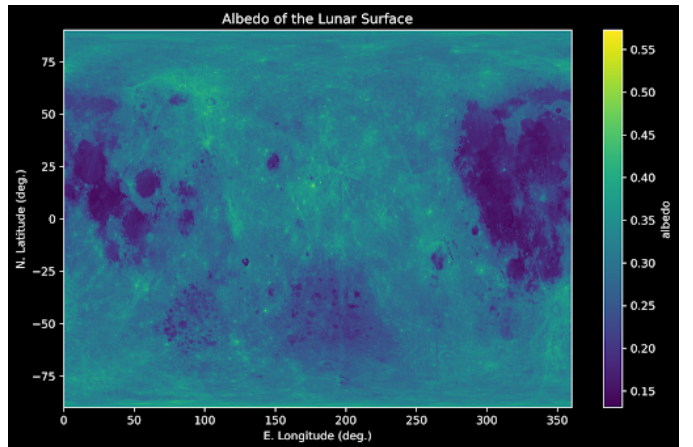


Figure 5: This figure is visual representation of the measured albedo across the lunar surface. The x and y axes correspond to degrees of longitude and latitude respectively while the colorbar represents the albedo.

| | CBVC | Mare Imbrium | Mare Nectaris |
|---------------------|-------------|---------------------|----------------------|
| μ (milligal) | 52.69 | 321.21 | 334.97 |
| σ (milligal) | 26.46 | 174.29 | 230.68 |

Table 1: Gravitational Characteristics of Lunar Regions: This table presents the calculated mean and standard deviation values of the gravitational measurements across different regions of the Moon in milligals.

| | CBVC | Mare Imbrium | Mare Nectaris |
|----------|-------------|---------------------|----------------------|
| μ | 0.35 | 0.21 | 0.25 |
| σ | 0.02 | 0.04 | 0.05 |

Table 2: Albedo Variability in Lunar Regions: This table summarizes the mean values and standard deviations for the albedo across the Compton-Belkovich Volcanic Complex and both Mare regions, providing insights into the reflective properties of these lunar surfaces.

3.2. Spectral Analysis

Following our spectral analysis of the lab samples of tectosilicate plagioclase feldspar, iron oxide, olivine, and augite compared to the Moon Mineralogy Mapper Data, we found the mixing coefficients (Table 3). We also plotted the spectra of the lab samples against a model spectra and the actual observed reflectance for each region of interest (Figures 7-9).

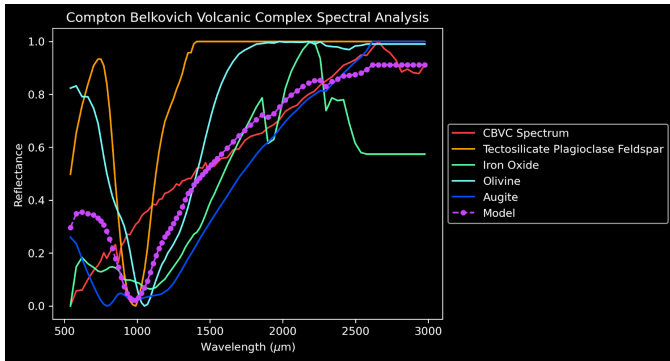


Figure 7: This figure displays spectra of the lab samples of tectosilicate plagioclase feldspar, iron oxide, olivine, and augite compared to our model data and the Moon Mineralogy Mapper Data for the CBVC. The y-axis is reflectance and the x-axis is wavelength in units of μm .

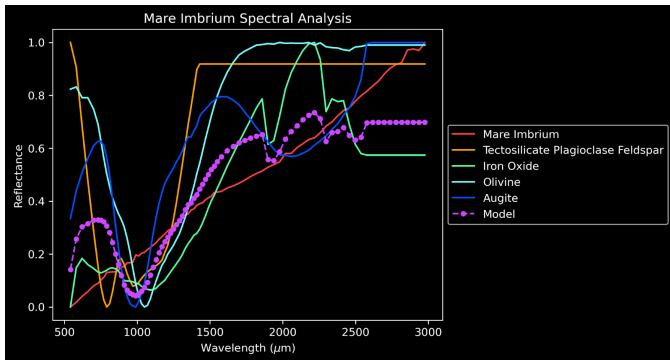


Figure 8: This figure displays spectra of the lab samples of tectosilicate plagioclase feldspar, iron oxide, olivine, and augite compared to our model data and the Moon Mineralogy Mapper Data for Mare Imbrium. The y-axis is reflectance and the x-axis is wavelength in units of μm .

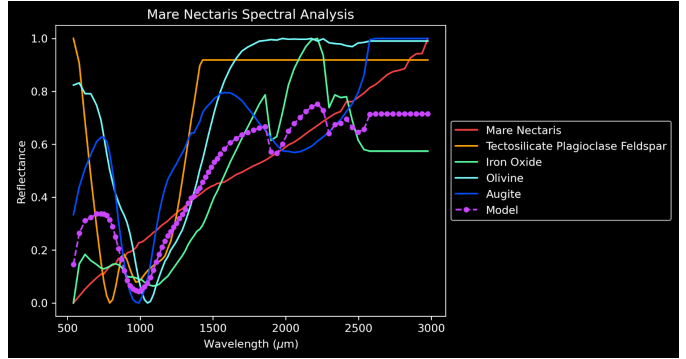


Figure 9: This figure displays spectra of the lab samples of tectosilicate plagioclase feldspar, iron oxide, olivine, and augite compared to our model data and the Moon Mineralogy Mapper Data for Mare Nectaris. The y-axis is reflectance and the x-axis is wavelength in units of μm .

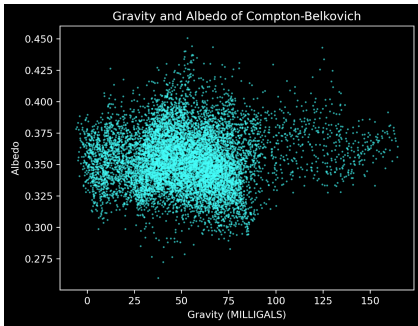
| Mineral | CBVC | Mare Imbrium | Mare Nectaris |
|-------------------|-------------|---------------------|----------------------|
| Feldspar | 33.1% | 0.0% | 0.0% |
| Iron Oxide | 11.5% | 52.8% | 52.6% |
| Olivine | 0.0% | 0.0% | 0.0% |
| Augite | 55.4% | 47.2% | 47.4% |

Table 3: Mineral Mixing Coefficients of Specified Lunar Regions: A quantitative representation of mineral composition in lunar regions based on lab sample analysis and Moon Mineralogy Mapper Data.

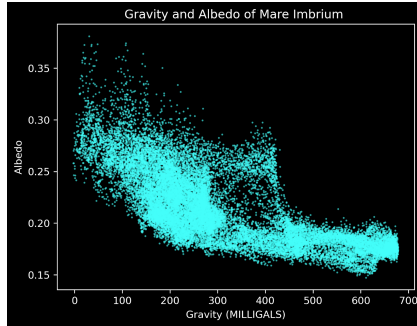
3.3. KREEP Elements

Finally, for each of the above regions, we analyzed the abundance of thorium and potassium. Our colormap scatter plot of results for these elemental abundances are shown in Figure 10. We found that at Compton-Belkovich Volcanic Complex, thorium reached a high of about 1.8 PPM between 56 and 58 degrees North Lat. and 97.5 and 100 Degrees East Long. In this same location, potassium reached a high value of over 800 PPM. For the Mare Imbrium, there was a maximum thorium concentration of over 8 PPM between 30 and 35 degrees North Lat. and near zero degrees East Long. In the same location, there was a maximum amount of potassium of about 3000 PPM. Finally, for the Mare Nectaris region, there was a maximum thorium concentration of around 1.5 PPM between -12 and -13 degrees North Lat. and between 34 and 36 degrees East Long. In this same location, we saw a maximum potassium concentration of over 675 PPM.

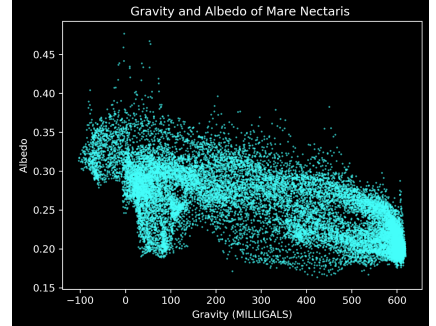
In addition to an analysis of KREEP elements, we also analyzed the abundance of silicon and oxygen at each of our regions. The results of this analysis are depicted in Figure 10. We found that at the Compton-Belkovich Volcanic Complex, silicon reached a maximum concentration of over 210,000 PPM between 52 and 54 Degrees North Lat. and roughly 100 degrees East Long. Oxygen reached a maximum concentration of about 457,500 PPM between 56 and 58 degrees North Lat. and at about 90 degrees East Long. At the Mare Imbrium, silicon reached a maximum concentration of over 180,000 PPM between 30 and 35 degrees North Lat., 0 and 10 degrees East Long., and 35 and 40 degrees North Lat., -20 and -10 degrees East Long. Oxygen reached a maximum concentration of over



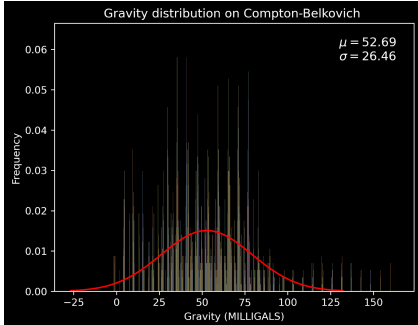
(a) This displays the correlations between positive gravity anomalies and the surface albedo of the CBVC.



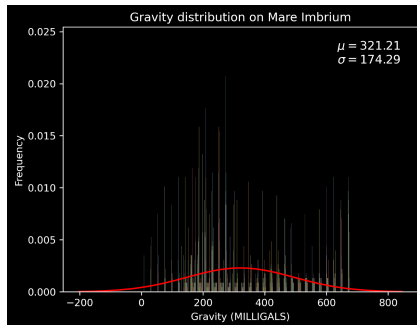
(b) This displays the correlations between positive gravity anomalies and the surface albedo of Mare Imbrium.



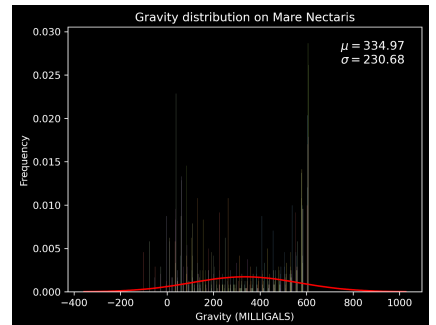
(c) This displays the correlations between positive gravity anomalies and the surface albedo of Mare Nectaris.



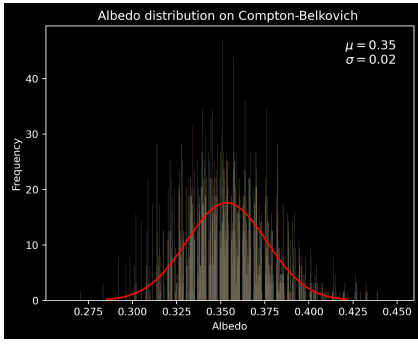
(d) This displays the normalized gravity distribution of the CBVC.



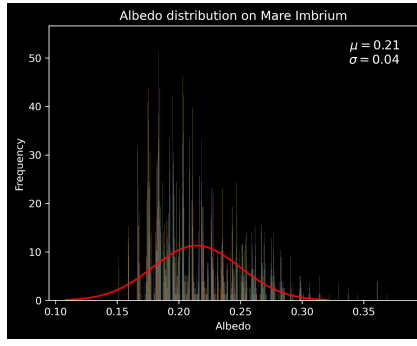
(e) This displays the normalized gravity distribution of Mare Imbrium.



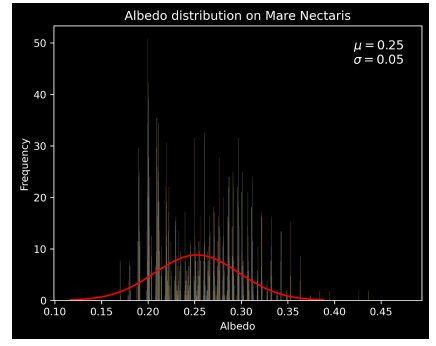
(f) This displays the normalized gravity distribution of Mare Nectaris.



(g) This displays the normalized albedo distribution of the CBVC.



(h) This displays the normalized albedo distribution of Mare Imbrium.



(i) This displays the normalized albedo distribution of Mare Nectaris.

Figure 6: The 9 sub-figures shown above display visual results from our various gravitation and albedo analyses. For graphs 6.a-6.c, the y-axis is albedo and the x-axis is gravity in units of milligals. For graphs 6.d-6.f, the y-axis is frequency and the x-axis is gravity in units of milligals. For graphs 6.g-6.i, the y-axis is frequency and the x-axis is albedo.

435,000 PPM between 35 and 40 degrees North Lat. and -20 and -10 degrees East Long. Finally, at the Mare Nectaris region, silicon reached a maximum concentration of over 215,000 PPM between -12 and -13 degrees North Lat. and 34 and 36 degrees East Long. In the same region, oxygen reached a maximum concentration of over 456,000 PPM.

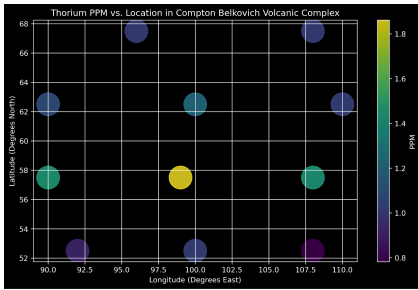
4. Discussion

4.1. Correlations Between Gravity and Albedo Across the Lunar Surface

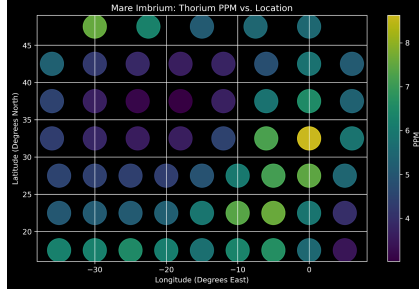
Gravity anomalies are a significant identifier of silicic volcanism and differing interior structures. In gravitational analysis, as depth increases, the porosity of the lunar crust decreases and the density of the crust increases. This causes an increase

in density difference between silicic magma and the lunar crust. By identifying the areas of high gravitational difference, we can find where silica structures are present in the interior.

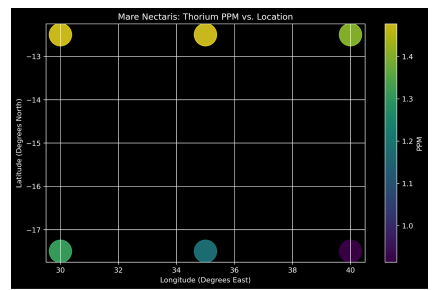
The correlations of distributions of the Compton-Belkovich Volcanic Complex, Mare Imbrium, and Mare Nectaris indicate that there are interior and compositional differences that would lead to evidence of silicic volcanism. By comparing the distribution of the albedo and the gravity differences at each region, we can make comparisons between these regions (Figure 6). The gravity measurements are the differences in the measured gravity at that location and the expected gravity at that given area at that elevation. In each of the regions, there is a peak in gravity that is greatly above the mean and standard deviation of the data. In the Mare Imbrium and Mare Nectaris, the peak in gravity is between 600-700 milligals. The peak in



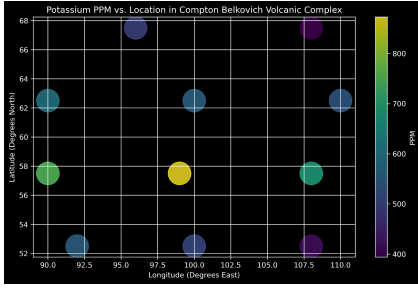
(a) This displays the concentration of thorium in the CBVC.



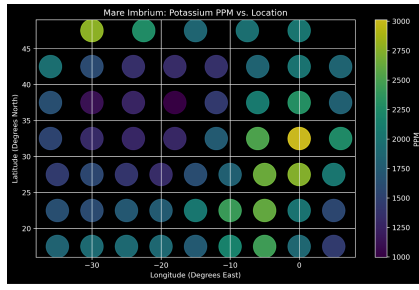
(b) This displays the concentration of thorium in Mare Imbrium.



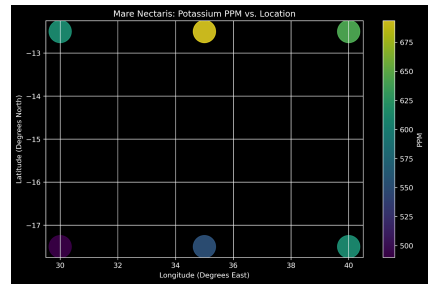
(c) This displays the concentration of thorium in Mare Nectaris.



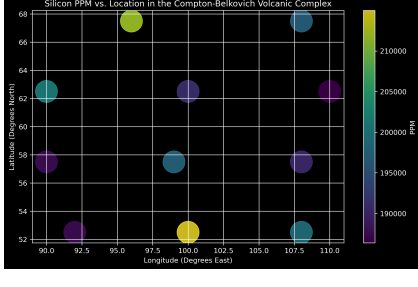
(d) This displays the concentration of potassium in the CBVC.



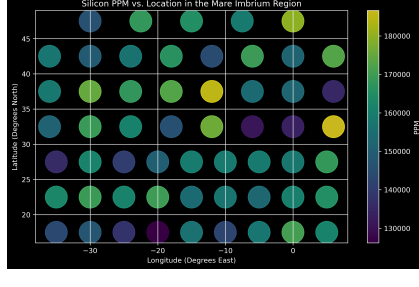
(e) This displays the concentration of potassium in Mare Imbrium.



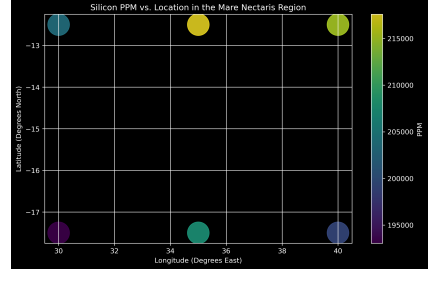
(f) This displays the concentration of potassium in Mare Nectaris.



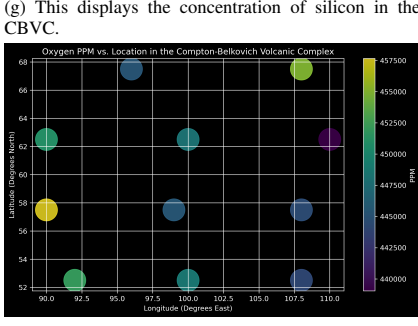
(g) This displays the concentration of silicon in the CBVC.



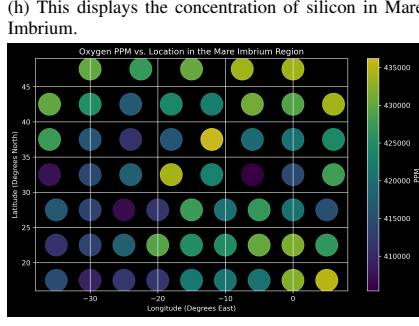
(h) This displays the concentration of silicon in Mare Imbrium.



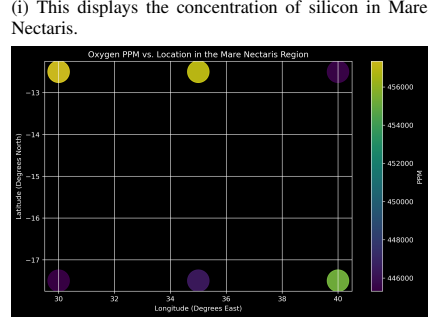
(i) This displays the concentration of silicon in Mare Nectaris.



(j) This displays the concentration of oxygen in the CBVC.



(k) This displays the concentration of oxygen in Mare Imbrium.



(l) This displays the concentration of oxygen in Mare Nectaris.

Figure 10: The above sub-figures display our analysis of KREEP elemental abundances as well as oxygen and silicon. Figures 10.a-10.c, show the thorium concentration as PPM represented by the colorbar at specific points of latitude and longitude, which are the y and x axes respectively. Figures 10.d-10.f display potassium, 10.g-10.i display silicon, and 10.j-10.l display the oxygen; all of these sub-figures have the same set up for axes labels and colorbar representations.

gravity for the CBVC is lower than the Mare regions because Compton-Belkovich is a volcanic complex while the Mare regions are calderas. By identifying these areas that have peaks at high gravitational differences, it can be concluded that there are features underneath the surface of the Moon, causing these gravitational differences to be much higher than expected.

Looking at the albedo distribution led to conclusions about the composition of material in the regions specified. Higher albedos are indications of materials with higher reflective prop-

erties. Silicate has higher albedo than other common materials found on the surface so it is evident that regions of higher albedos contain a higher abundance of silicic materials, which is also supported by spectral analysis. Looking at Table 2, the Compton-Belkovich Volcanic Complex has a greater mean albedo value than the Mare regions because of the higher quantity of cooled basaltic material that makes up the majority of these Mare regions. However, the crustal regions, i.e. the region that outlines the Mare, is where the higher albedo is con-

sistently present, and this is observed through the albedo map (Figure 2) of the lunar surface and visible light images. The Compton-Belkovich Volcanic Complex is not part of a caldera region, rather it is its own volcanic dome in a highly cratered area, observed by visible images. Once again, the presence of a larger abundance of higher albedos in this area indicates that there are compositional differences between these locations and their surrounding areas, which is confirmed by spectral analysis.

4.2. Complex Spectral Analysis

The spectral analysis of the Compton-Belkovich Volcanic Complex, Mare Imbrium, and Mare Nectaris provides evidence of silicic volcanism occurring at each site. Each region exhibited high compositional abundances of silicon and silicate-based materials. We chose to look at the spectra of tectosilicate plagioclase feldspar due to this being a common compound found in lunar basalt samples. Olivine is an element that we expect to see in both silicic and basaltic magma due to its composition of $(\text{Mg}_2\text{Fe}_2) \text{SiO}_4$. Magnesium and iron are highly abundant in mafic (basaltic) magma while silicon and oxygen are highly abundant in felsic (silicic) magma. Additionally, augite is an inosilicate found in silicic material and iron oxide is a compound that exists in high quantities in mafic (basaltic) magma and lesser quantities in silicic magma. Based on the compositions of these compounds, we would expect to see high concentrations of the silicate based compounds such as augite, olivine, and tectosilicate plagioclase feldspar and lower concentrations of iron oxide in our regions, assuming past silicic volcanism.

Our results (Table 3) indicate that the Compton-Belkovich Volcanic Complex is composed of 88% compounds high in silicon and oxygen. These are elements that are expected to make up over 60% of silicic magma. Because we do not know the exact amount of silicon or oxygen in these samples, but only that there is a high compositional abundance of materials containing these elements, we are not surprised to find over 60% of the region composed of silicic material. Additionally, if silicic volcanism is present, we expect to see lunar spectra that are similar to the above lab spectra. Looking at the Compton-Belkovich Volcanic Complex, we do in fact see a spectrum very similar to a combination of tectosilicate plagioclase feldspar and augite. In the same way, looking at the Mare Imbrium and Mare Nectaris regions, the lunar spectra is most similar to the spectra of iron oxide and augite.

The models for each lunar spectra (Figures 7-9) display what we expect the lunar spectra to look like based on the mixing coefficients. These mixing coefficients are limited to the four compounds we looked at, which undoubtedly do not explain the entire composition of the lunar surface. Because the lunar surface is composed of more than these four compounds, our model did not fit the spectra perfectly. The biggest difference between the lunar spectra and lab spectra for all three regions, indicated by the difference between the model and actual lunar data, is the lack of an absorption band around 1000 angstroms. This could explain why we see a 0.0% mixing coefficient for olivine in all three regions, a compound we ex-

pect to see a higher abundance of for both basaltic and silicic magma. Space weathering could be a solution to this problem. Maturation of the lunar surface due to space weathering affects the way that light is both absorbed and reflected. More specifically, space weathering can lead to reduced contrast in absorption bands (Denevi et al. (2023)). Because we are analyzing lunar mare and volcanoes, this surface is very old and thus has experienced extensive space weathering processes. This weathering has likely caused the erasure of the absorption band at 1000 Angstroms, causing our analysis to identify 0.0% olivine and tectosilicate plagioclase feldspar at Mare Nectaris and Mare Imbrium. Additionally, this may have affected the compositional coefficients at the Compton-Belkovich Volcanic Complex, causing there to be 0.0% olivine when in reality, we assume this value to be higher.

Differences in the mineral compositions between the Compton-Belkovich and mare regions include a variance in the iron oxide we were able to spectrally detect. The mare regions showed similar FeO_2 compositions (52.8% and 52.6%), while the Compton-Belkovich region exhibited a notably lower composition at 11.5%. This indicates that the volcanism in the mare regions was more basaltic than that in the Compton-Belkovich region we studied, suggesting that these regions underwent varying conditions during volcanic formation. Interestingly, augite is similarly present across all regions, suggesting there were also similarities in their volcanic histories. These similarities and differences may be crucial in revealing the volcanic evolution of the Moon. Variations across lunar landscapes could indicate influences from local conditions and the times at which they formed, among a multitude of factors

4.3. Abundance of KREEP Elements

Based on our analysis of silicon and oxygen abundances in each of our lunar regions in addition to the spectral analysis, we can conclude that silicic volcanism has occurred to some extent at each of our regions. Figure 10 displays the abundance of these elements in each region. Although the spectra at the Mare Imbrium and Mare Nectaris regions may indicate that the volcanism was a combination of both silicic and basaltic magma, we can conclude that silicic volcanism did occur due to the high abundance of silicon and oxygen in these regions. Our data show that the silicon concentration in each of our regions ranged from 180,000 to 215,000 PPM, and oxygen concentrations ranged from 435,000 to 457,500 PPM. These high concentrations indicate the existence of silicic magma in each region. Drawing the conclusion that the Compton-Belkovich Volcanic Complex, Mare Imbrium, and Mare Nectaris all exhibit silicic volcanism, we are able to continue our analysis as to why this volcanism may have occurred in the absence of tectonic plates and water. Analyzing each of our regions for KREEP elements, we can determine whether the existence of such elements may have been a driving force behind the formation of silicic magma.

Based on our analysis of thorium and potassium abundances in each of the lunar regions, we expect that silicic magma occurred due to radiogenic heating of KREEP elements. KREEP

elements include potassium, rare earth elements such as thorium, and phosphorus. We chose to analyze thorium and potassium abundances specifically because this data was readily available via Lunar Prospector Reduced Spectrometer Data, and because much research has been done to explain the thorium anomaly at the Compton-Belkovich Volcanic Complex. Our data show that there are high abundances of both thorium and potassium in each of the regions we analyzed. The presence of these elements could have allowed for partial heating below the crust due to radioactive decay. Scientists have previously predicted the existence of a contemporary upper-mantle melt zone (Grimm (2013)) where radioactive decay of KREEP elements such as potassium, thorium, and uranium transferred heat into the lunar upper-mantle that allowed for multi-stage partial melting of the lunar crust. This partial melting allowed for the formation of silicic magma.

To prove our hypothesis that KREEP elements contributed to the partial heating of silicic magma, we needed to show that there was a high concentration of these elements at each of our volcanic regions. As shown in the above figures, the maximum thorium concentrations ranged between 1.2 and 8 PPM in each of the analyzed regions. This is comparable to around 0 PPM for other regions of the Moon. The maximum potassium concentrations ranged between 675 and 3000 PPM, again comparable to approximately 0 PPM in non-volcanic regions. These abnormally high concentrations of KREEP elements visible in areas of past silicic volcanism indicate that the radiogenic heating from KREEP elements may have been a key factor in the formation of silicic magma on the Moon.

4.4. Hypothesis Analysis, Possible Shortcoming

Initially, we hypothesized that radiogenic heating of KREEP elements in addition to crustal remelting caused by impact cratering allowed for the formation of silicic magma on the Moon. After beginning our analysis, we were unable to draw conclusions about the effect of crustal melting due to impact cratering. This was due to a lack of time that would have been needed to analyze the number of impact craters at each region. Due to this lack of analysis, we are unable to conclude that the radiogenic heating of KREEP elements was the main contributor to partial heating of silicic magma beneath the lunar surface. We therefore advise future researchers to focus on the potential effects that impact cratering may have had on heat transfer into the upper mantle, as this transfer of heat may have worked in conjunction with radiogenic heating to form silicic magmas.

5. Conclusion

In conclusion, by analyzing three key lunar features—the Compton-Belkovich Volcanic Complex, Mare Nectaris, and Mare Imbrium—and employing a multidisciplinary approach that includes gravity and albedo measurements, spectral analysis, and KREEP element abundances, we confirmed the presence of silicic materials in all three regions. We also found Mare Nectaris and Mare Imbrium to be more basaltic in nature compared to the Compton-Belkovich Volcanic Complex.

5.1. Gravity and Albedo

We identified gravitational peaks across all three areas of interest for silicic volcanism. These peaks are indicative of high-density pockets of silicic material beneath the Moon's crust, reinforcing the theory of subsurface silicic structures likely formed by silicic volcanic activity. Albedo measurements showed higher reflectivity in areas correlated with these gravitational anomalies. This heightened reflectivity suggests that silicic materials, which exhibit greater reflectance, are present in higher quantities than in the surrounding basaltic landscapes. This finding underscores the unique composition of these silicic regions. The observed correlations between gravity and albedo, particularly the negative correlations in the mare regions compared to the Compton-Belkovich Volcanic Complex, illuminate differences in geological compositions. The mare regions, displaying a stronger and more uniform correlation between gravity and albedo, could indicate differences in volcanic activity between the mares and CBVC. Lower albedo measurements in the two mare regions compared to the CBVC support the idea that the mares are more basaltic.

5.2. Spectral Analysis

We conducted spectral analysis in all of our regions and on four key materials: tectosilicate plagioclase feldspar, iron oxide, olivine, and augite, to investigate the presence of silicic volcanism. Our analysis identified the presence of feldspar, iron oxide, and augite, substantiating the existence of past silicic volcanism at the Compton-Belkovich Volcanic Complex. Notably, while olivine is typically expected in areas of silicic volcanism, it showed a 0% mixing coefficient, indicating a complete absence in the spectrum analyzed. This absence could highlight a unique aspect of volcanic activity in this area.

Both Mare Nectaris and Mare Imbrium showed similar mixing coefficients for iron oxide and augite but exhibited an absence of feldspar and olivine. The similarities in these compositions suggest that these regions might have similar volcanic histories.

The absence of expected materials, such as olivine in all regions and tectosilicate plagioclase feldspar in the mares, could likely be caused by space weathering easing the absorption bands of interest in our spectral analysis. The two mares have a higher iron oxide mixing coefficient compared to the CBVC area, which supports the idea that the mares are more basaltic than the CBVC area.

5.3. KREEP Elements

Finally, we examined the composition of KREEP elements—potassium, rare earth elements, and phosphorus—in these three areas of interest. We found high concentrations of KREEP elements in all areas, reinforcing their critical role in the formation of silicic magmas. Our analysis confirmed significant concentrations of thorium and potassium, specifically. The presence of these KREEP elements supports the hypothesis that radiogenic heating from their radioactive decay contributed to the formation of silicic magmas by causing partial melting of

the lunar crust. This heating mechanism is particularly significant in inducing volcanic activity on the Moon, which lacks plate tectonics. Our findings suggest that KREEP elements are a fundamental factor in the thermal history of the Moon's crust and have significantly contributed to the Moon's volcanic history.

5.4. Future Research

The first area of focus for future research would be to investigate the significance of impact cratering on the presence of silicic materials. By exploring how heat transfer from impact cratering may cause partial melting of the Moon's crust and form silicic materials, then comparing it to the abundance of KREEP elements may discern any insights about the contribution of both heating mechanisms.

Conducting a more comprehensive study of different types of lunar features would also improve the clarity of our findings. By comparing mixing coefficients, gravity and albedo correlations, and KREEP element concentrations across as many lunar features as possible may provide conclusions about trends that could exist among similar or dissimilar topographies. This effort could be extended further by creating a multidisciplinary dataset for lunar mapping. Developing an easy-to-navigate model incorporating all three types of information could make future research more accessible.

Additionally, machine learning presents an intriguing area of interest. Creating an algorithm that automates many of the processes we underwent to analyze data gathered from instruments, may further accelerate the discovery of trends and leverage predictions of the properties of geological features and perhaps volcanism occurring on similar moons and other planetary bodies.

6. Acknowledgements and Author Contributions

6.1. Acknowledgements

We express our gratitude to Professor Paul Hayne for his guidance on gravitational, spectral, and KREEP analyses, and for his assistance in sourcing invaluable data from NASA's Planetary Data System and other online resources. Additionally, we would like to acknowledge our peer reviewers—Brian Balajonda, Tyler Curnow, Maximus Montano, and Trever Sotostanti—who provided valuable feedback during the rough draft stage of our research paper. For coding help and other general questions, we thank our laboratory assistant, Eli Monyek, for being an indispensable resource both during class and in office hours.

Furthermore, we utilized several online resources for coding assistance, including Python documentation for initial inquiries and information on the spectral Python module. ChatGPT was also instrumental in addressing specific coding questions and identifying coding errors.

6.2. Author Contributions

Elena Carlson analyzed the spectral data from the Compton-Belkovich Volcanic Complex and created figures for both lab and Moon Mineralogy Mapper data. She also completed the analysis of potassium and thorium abundances for all three regions, creating scatter plots of potassium and thorium abundance versus location. Elena wrote the methodologies, results, and discussion sections on spectral analysis and elemental abundance analysis of the paper. She also created the presentation used for sharing our findings with our peers and aided in the editing of this final paper.

Shaughnessy Dunn analyzed the distribution of gravity and albedo across all regions, creating histograms and scatter plot figures. She also produced images displaying the gravity and albedo of the entire lunar surface and wrote the methodology section concerning these aspects. Shaughnessy wrote the discussion section on the results of the gravity and albedo analysis and assisted in the creation of the presentation. Finally, she compiled the citations for the bibliography.

Taylor Hagerman initially analyzed element abundance and spectral data in relation to location-based image data, but this approach was abandoned due to challenges in accessing sufficiently detailed image data. Instead, she created scatter plots for oxygen and silicon abundance versus location. Taylor wrote the introduction section of the paper, edited the abstract, and revised discussions based on prior research. They also wrote all figure and table captions included in the paper. She conducted final editing and formatting of the paper using Overleaf.

Izzy Perez analyzed spectral data from Mare Imbrium and Mare Nectaris, creating figures for both lab and Moon Mineralogy Mapper data. She organized and formatted the shared slide deck document and assisted with the overall organization of the paper. Izzy wrote the abstract, the conclusion, and the concluding paragraph of the spectral discussion comparing the mares to the CBVC area. She wrote the acknowledgment and author contribution section as well as providing final editing and formatting of the paper using Overleaf.

References

- Andrews-Hanna, J. C., Besserer, J., Head III, J. W., Howett, C. J., Kiefer, W. S., Lucey, P. J., McGovern, P. J., Melosh, H. J., Neumann, G. A., Phillips, R. J., Schenk, P. M., Smith, D. E., Solomon, S. C., & Zuber, M. T. (2014). Structure and evolution of the Lunar Procellarum region as revealed by Grail Gravity Data. *Nature*, 514(7520), 68–71. <https://doi.org/10.1038/nature13697>
- Ashley, J. W., Robinson, M. S., Stopar, J. D., Glotch, T. D., Hawke, B. R., van der Bogert, C. H., Hiesinger, H., Lawrence, S. J., Jolliff, B. L., Greenhagen, B. T., Giguere, T. A., & Paige, D. A. (2016). The lassell massif—a silicic lunar volcano. *Icarus*, 273, 248–261. <https://doi.org/10.1016/j.icarus.2015.12.036>
- Boyce, J. M., Giguere, T., Mouginis-Mark, P., Glotch, T., & Taylor, G. J. (2018). Geology of Mairan Middle Dome: Its implication to Silicic volcanism on the Moon. *Planetary and Space Science*, 162, 62–72. <https://doi.org/10.1016/j.pss.2017.12.009>
- Clegg-Watkins, R. N., Jolliff, B. L., Watkins, M. J., Coman, E., Giguere, T. A., Stopar, J. D., & Lawrence, S. J. (2017). Nonmare volcanism on the Moon: Photometric evidence for the presence of evolved silicic materials. *Icarus*, 285, 169–184. <https://doi.org/10.1016/j.icarus.2016.12.004>

- Denevi, B. W., Noble, S. K., Christoffersen, R., Thompson, M. S., Glotch, T. D., Blewett, D. T., Garrick-Bethell, I., Gillis-Davis, J. J., Greenhagen, B. T., Hendrix, A. R., Hurley, D. M., Keller, L. P., Kramer, G. Y., & Trang, D. (2023). Space weathering at the Moon. *Reviews in Mineralogy and Geochemistry*, 89(1), 611–650. <https://doi.org/10.2138/rmg.2023.89.14>
- Glotch, T. D., Lucey, P. G., Bandfield, J. L., Greenhagen, B. T., Thomas, I. R., Elphic, R. C., Bowles, N., Wyatt, M. B., Allen, C. C., Hanna, K. D., & Paige, D. A. (2010). Highly Silicic compositions on the Moon. *Science*, 329(5998), 1510–1513. <https://doi.org/10.1126/science.1192148>
- Goossens, S., Sabaka, T. J., Wieczorek, M. A., Neumann, G. A., Mazarico, E., Lemoine, F. G., Nicholas, J. B., Smith, D. E., & Zuber, M. T. (2020). High-Resolution Gravity Field models from Grail data and implications for models of the density structure of the Moon's crust. *Journal of Geophysical Research: Planets*, 125(2). <https://doi.org/10.1029/2019je006086>
- Greenhagen, B. T., Lucey, P. G., Wyatt, M. B., Glotch, T. D., Allen, C. C., Arnold, J. A., Bandfield, J. L., Bowles, N. E., Hanna, K. L., Hayne, P. O., Song, E., Thomas, I. R., & Paige, D. A. (2010). Global silicate mineralogy of the Moon from the diviner lunar radiometer. *Science*, 329(5998), 1507–1509. <https://doi.org/10.1126/science.1192196>
- Grimm, R. E. (2013). Geophysical constraints on the lunar Procellarum KREEP Terrane. *Journal of Geophysical Research: Planets*, 118(4), 768–778. <https://doi.org/10.1029/2012je004114>
- Gullikson, A. L., Hagerty, J. J., Reid, M. R., Rapp, J. F., & Draper, D. S. (2016). Silicic lunar volcanism: Testing the crustal melting model. *American Mineralogist*, 101(10), 2312–2321. <https://doi.org/10.2138/am-2016-5619>
- Ivanov, M. A., Head, J. W., & Bystrov, A. (2016). The lunar Gruithuisen Silicic extrusive domes: Topographic configuration, morphology, ages, and internal structure. *Icarus*, 273, 262–283. <https://doi.org/10.1016/j.icarus.2015.12.015>
- Jolliff, B. L., Wiseman, S. A., Lawrence, S. J., Tran, T. N., Robinson, M. S., Sato, H., Hawke, B. R., Scholten, F., Oberst, J., Hiesinger, H., van der Bogert, C. H., Greenhagen, B. T., Glotch, T. D., & Paige, D. A. (2011). Non-mare silicic volcanism on the Lunar Farside at Compton–Belkovich. *Nature Geoscience*, 4(8), 566–571. <https://doi.org/10.1038/ngeo1212>
- Kiefer, W. S., Taylor, G. J., Andrews-Hanna, J. C., Head, J. W., Jansen, J. C., McGovern, P. J., Robinson, K. L., Wieczorek, M. A., & Zuber, M. T. (n.d.). The bulk density of the small lunar volcanoes Gruithuisen Delta and Hansteen Alpha: Implications for volcano composition and petrogenesis. NASA/ADS. <https://ui.adsabs.harvard.edu/abs/2016LPI....47.1722K/abstract>
- Liang, F., Amrouche, M., Yan, J., & Saibi, H. (2024). Detection of subsurface density structures of the Aristarchus Plateau by gravity inversion. *Journal of Geophysical Research: Planets*, 129(2). <https://doi.org/10.1029/2023je007856>
- Pigue, L. M., Bennett, K. A., Horgan, B. H., & Gaddis, L. R. (2023). Relationship between explosive and effusive volcanism in the Montes Apenninus region of the Moon. *Journal of Geophysical Research: Planets*, 128(11). <https://doi.org/10.1029/2023je007861>
- Qiu, D., Sasaki, S., Yan, J., Ye, M., Deng, Q., Liang, F., Liu, L., & Li, F. (2023). Buried Silicic volcanoes discovered in the Gruithuisen region on the Moon. *Geophysical Research Letters*, 50(11). <https://doi.org/10.1029/2023GL103336>
- Qiu, D., Ye, M., Yan, J., Zheng, C., Xiao, Z., Zhang, Q., Gao, W., Liu, L., & Li, F. (2022). New view of the lunar silicic volcanism in the mons hansteen: Formation and origins. *Journal of Geophysical Research: Planets*, 127(8). <https://doi.org/10.1029/2022je007289>
- Siegler, M. A., Feng, J., Lehman-Franco, K., Andrews-Hanna, J. C., Economos, R. C., Clair, M. St., Million, C., Head, J. W., Glotch, T. D., & White, M. N. (2023). Remote detection of a lunar granitic batholith at Compton–Belkovich. *Nature*, 620(7972), 116–121. <https://doi.org/10.1038/s41586-023-06183-5>
- Su, B. (2023, June 16). Crustal remelting origin of highly silicic magmatism on the Moon. figshare. <https://doi.org/10.6084/m9.figshare.23244101>
- Valencia, S., Watkins, R. N., Richardson, J. A., Glotch, T., Jawin, E., Ravi, S., & Jolliff, B. L. (2021). End-member volcanism in the absence of plate tectonics: Silicic volcanism on the Moon. *Bulletin of the AAS*, 53(4). <https://doi.org/10.3847/25c2feb.ea66ecb8>
- Whitaker, E. A. (1972). Lunar color boundaries and their relationship to topographic features: A preliminary survey. *The Moon*, 4(3–4), 348–355. <https://doi.org/10.1007/bf00562002>
- Wilson, J. T., Eke, V. R., Massey, R. J., Elphic, R. C., Jolliff, B. L., Lawrence, D. J., Llewellyn, E. W., McElwaine, J. N., & Teodoro, L. F. (2015). Evidence for explosive silicic volcanism on the Moon from the extended distribution of thorium near the Compton–Belkovich Volcanic Complex. *Journal of Geophysical Research: Planets*, 120(1), 92–108. <https://doi.org/10.1002/2014je004719>
- Wilson, L., & Head, J. W. (2003). Lunar Gruithuisen and mairan domes: Rheology and mode of emplacement. *Journal of Geophysical Research: Planets*, 108(E2). <https://doi.org/10.1029/2002je001909>